Indian J. Phys. **49**, 287–295 (1975)

Charge transport in a Van de Graaff generator

ASHIM KUMAR GANGULY AND ASOK SAHA*

Saha Institute of Nuclear Physics, Calcutta 700009

(*Received* 4 *September* 1974, *revised* 1 *February* 1975)

Experiments were performed with a Van de Graaff generator under atmospheric conditions on different comb configurations and their geometries in order to obtain informations on their relative performances and to identify the factors responsible for efficient transport of charges to the high voltage terminal. A maximum short circuit current of $\sim 120\,\mu A$ with a charge carrying efficiency of 75% was achieved.

1. INTRODUCTION

While constructing a Van de Graaff accelerator in the 1 MeV range (Chatterjee *et al* 1973) for nuclear reaction work, we found that various arrangements of corona combs for spraying and collection of charges have been reported in the literature (Van Atta *et al* 1936, Smee 1944, Van de Graaff *et al* 1946, Craggs & Meek 1954, Herb 1959, Livingston & Blewett 1962). But apart from some statements and prescriptions regarding the arrangements and positions of these corona combs, very little published quantitative information is available as to the comparative performances for changes in the arrangements of the combs and the variation in their geometries around the prescribed ones. We therefore undertook intensive studies under atmospheric conditions on relative performances of different comb configurations and their geometries for optimization of the charge transport to the high voltage terminal. Some of the results have been briefly reported elsewhere (Ganguly & Saha 1973).

2. EXPERIMENTAL SETUP AND RESULTS

The investigations were carried out in a test setup reported earlier (Chatterjee *et al* 1973) which is shown schematically in figure 1. A 18 cm wide × 3 mm thick endless nylon woven belt mounted on two 8 cm dia. solid mild steel rollers, one each at ground and high voltage ends, was driven by a 3 phase 2 H.P. motor at a linear speed of 1300 metres/min. Corona combs were made of $\frac{1}{2}''$ long gramophone needles fixed on a $\frac{1}{2}''$ dia. brass rod, the distance between two adjacent needles was 1/4″. The experiments were carried out under atmospheric conditions at a mean room temperature ~28°C with a mean relative humidity ~ 60%. The temperature and relative humidity remained practically around the above mentioned values for all the sets of experiments performed.

* Present address : Nuclear Physics Laboratory, Bose Institute, Calcutta 700 009.

2.1. *Arrangement of combs :* For charging and discharging the belt with the help of corona combs, one normally uses one (Smee 1944, Van de Graaff *et al* 1946), or two (Livingston & Blewett 1962) combs at the ground end for positive charge spraying and negative charge collection; and one (Herb 1959), two (Smee 1944), or three (Herb 1959) combs at the high voltage end for positive charge collection and negative charge spraying and their control. We studied various possible arrangements of combs in our setup upto two combs at the ground end and three combs at the high voltage end to find out the relative performances in each case. These comb configurations are represented by the various positions of the four schematic switches of figure 1 and are listed in table 1.

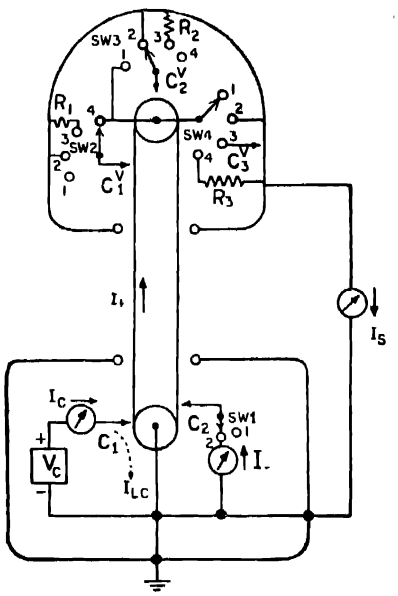

Fig. 1. Experimental arrangement

C_1, C_2 : ground end corona combs; V_C : ground end spray voltage; I_C : ground end spray current : I_+ : current due to charges going up with the belt; I_- : current due to charges coming down with the belt and collected by the comb C_2; I_S : short circuit current; C_1^V, C_2^V, C_3^V: corona combs inside the dome; R_1, R_2, R_3 : Resistances inside the dome; d_{C_1}, d_{C_2} : distnces of the combs C_1, C_2 respectively from the ground end base plate; d_{CR_1}, d_{CR_2} : distances of the combs C_1, C_2 respectively from the ground end roller centreline; d_R : distance of the ground end roller centreline from the ground end base plate; $d^V{}_{C_1}$: distance the comb C_1^V from the dome base plate; d_R^V : distance of the dome end roller centreline from the dome base plate ; g_1, g_2, g_1^V, g_2^V : static gaps between the belt and needle tips of the combs C_1, C_2, C_1^V, C_2^V respectively; g_3^V: gap between the dome surface and the needle tips of the comb C_3^V; SW1, SW2, SW3, SW4 : schematic switches. The different comb configurations can be arrived at by altering the positions of these switches.

Table 1. Comb configurations

Config. No.	Configuration	Config. No.	Configuration	Config. No.	Configuration
I.1	(1) (2) (4) (1)	I.12a	(1) (1) (1) (1) Ex	II.9	(2) (1) (3) (1)
I.2	(1) (2) (4) (2)	I.13	(1) (1) (1) (4)		
I.3	(1) (3) (4) (1)	I.13a	(1) (1) (1) (4) Ex	III.1	(1) (2) (2) (1)
I.4	(1) (4) (4) (4)	I.14	(1) (1) (3) (1)	III.1*a*	(1) (2) (2) (1) Ex
I.5	(1) (4) (4) (1))	I.14a	(1) (1) (3) (1) Ex	III·2	(1) (4) (2) (1)
I.6	(1) (3) (4) (2)			III.2a	(1) (4) (2) (1) Ex
I.7	(1) (2) (4) (4)	II.1	(2) (2) (4) (2)		
I.8	(1) (1) (2) (1)	II.2	(2) (2) (4) (1)	IV.1	(2) (2) (2) (1)
I.8a	(1) (1) (2) (1) Ex	II.3	(2) (1) (2) (2)	IV.2	(2) (4) (2)) 1)
I.9	(1) (1) (2) (2)	II.3a	(2) (1) (2) (2) Ex	IV.2a	(2) (4) (2) (1) Ex
I.9a	(1) (1) (2) (2) Ex	II.4	(2) (1) (2) (1)	IV.3	(2) (4) (2) (4)
I.10	(1) (1) (3) (2)	II.4a	(2) (1) (2) (1) Ex	IV.4	(2) (4) (2) (2)
I.10a	(1) (1) (3) (2) Ex	II.5	(2) (1) (3) (2)	IV.5	(2) (4) (3) (1)
I.11	(1) (1) (2) (4)	II.6	(2) (1) (2) (4)		
I.11a	(1) (1) (2) (4) Ex	II.7	(2) (1) (1) (1)	V.1	(2) (4) (2) (3)
I.12	(1) (1) (1) (1)	II.8	(2) (1) (1) (4)		

Note : *Config. IV.2a* = (2)(4)(2)(1)*Ex* means switches SW1, SW2, SW3 and SW4 are respectively in positions 2, 4, 2 & 1; and (in cases where *Ex* is present) there are some adjustable extra needles in the comb C_2^V directed to the roller.

The short circuit current I_S which is the net current carried by the belt from the ground end to the dome with the dome grounded, was found to increase with the ground end spray current I_C and ultimately attained a saturation value in each of the comb configurations of types I-V studied. This saturation value of I_S indicates the maximum charge transfer for the particular comb configuration. Typical I_S vs I_C graphs for several configurations selected to cover the entire range of saturation short circuit currents observed are shown in figure 2. A histogram representing the saturation short circuit current for different comb configurations under a constant geometry determined by preliminary experiments is given in figure 3.

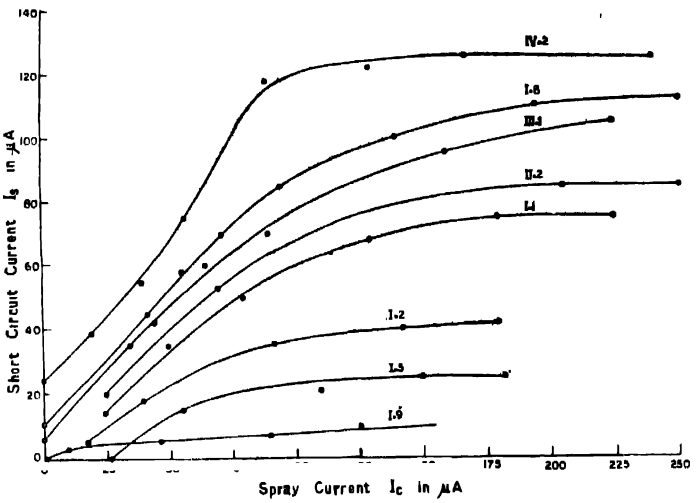

Fig. 2. Typical variation of the short circuit current I_S with the ground end spray current I_C showing the saturation attained in I_S. Configuration numbers are indicated against all the curves in the figure. In fact, saturation is attained in each of the comb configurations listed in table 1.

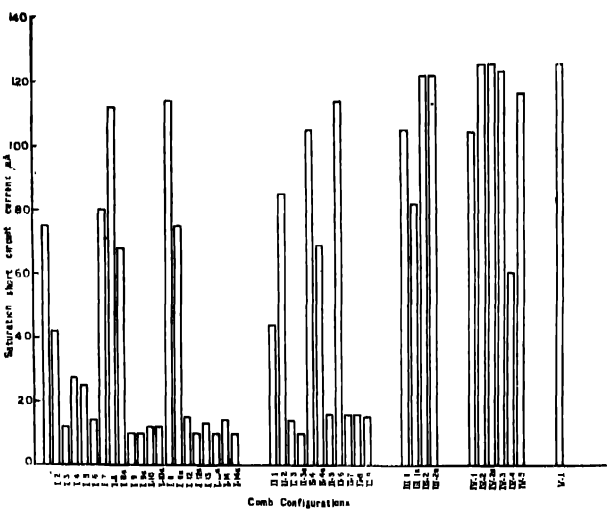

Fig. 3. Saturation short circuit currents for different comb configurations of table 1 for $d_{CR_1} = \frac{1}{2}''$; $g_1 = \frac{1}{2}''$; $d_{CR_2} = 2''$; $g_2 = \frac{1}{2}''$; $d^V{}_{C_1} = 1\frac{5}{8}''$; $g_1{}^V = \frac{1}{2}''$; $d_R{}^V = 2\frac{3}{4}''$; $g_R{}^V = \frac{1}{2}''$; $g^v{}_3 = 1''$. A maximum saturation short circuit current $\sim 120\mu A$ could be obtained.

From the comparative study of 21 cases of type I configuration (having one comb at the ground end and one comb inside the high voltage terminal) high-

lighting the basic features of charging and discharging mechanism of the belt the following conclusions become apparent :

(i) The high voltage end roller when connected to dome always yields lower currents. This is due to the fact that since the roller is at dome potential, the negative charge spraying is absent in this case.

(ii) The yield is very small when the comb C^V_1 or C^V_2 is connected to the roller. Charge transport to dome can only take place through leakages if any.

(iii) Additional needles on roller from the comb C^V_2 reduces the yield by draining away charges from the roller and thus limiting its voltage.

Addition of the comb C_2 at the ground end (type II configuration) did not alter the saturation short circuit current obtained in the corresponding type I configuration. However it has the useful effect of reducing the loading on the spray power supply by collecting the negative charges coming down which otherwise would have been neutralised by the spraying comb C_1. Thus in type II configuration, there is a reduction in I_C by an amount equal to I_- compared to the corresponding type I configuration.

Introduction of the second comb inside the high voltage terminal (type III configuration) increased the maximum saturation short circuit current from $114\mu A$ for type I configuration to about $125\,\mu A$. This was achieved when the comb C^V_1 was connected to the insulated roller. The second comb C_2 at the ground end in type IV arrangement as in type II case, reduces the loading on the spray power supply without affecting the maximum short circuit current.

Dome to roller potential difference is not only responsible for the collection of the incoming charge but is also responsible for spraying of the negative charge on the belt. By adjusting this voltage the magnitude of the incoming positive charges and outgoing negative charges can be made equal (Herb 1959). Hence an additional corona comb C^V_3 from roller to dome with an adjustable gap was added to configuration IV.2 to make configuration V.1.

2.2. *Comb geometry.* We selected out certain comb configurations for detailed study of comb positions, relative to the roller, belt surface etc., in order to ascertain the optimum geometry for efficient charge collection as indicated by maximum saturation short circuit current. Other configurations were not chosen because of lower yield and similarity of comb arrangements with these configurations. Since spraying and collection are completely independent processes, each separately controllable (Livingston & Blewett 1962) the ground end comb geometries which essentially control the spraying part and the high voltage end comb geometries which control the collection part (apart from negative charge spraying) were taken up separately.

(a) *Ground end :*

Studies at the ground end indicate that the saturation short circuit current is more or less independent of the ground end comb positions (d_{C_1}, d_{C_2}) and their gaps (g_1, g_2) as is evident from figure 4. The gap g_1 and the position d_{C_1} of the comb C_1 controls the threshold for the onset of corona. Relatively lower spray voltage is required when the gap g_1 is smaller and also when the distance d_{CR_1} from the centreline of the roller is smaller. But there is a minimum limit to d_{CR_1} below which frequent spark breakdown between the spraying comb and the roller occurs. Hence, apart from the variation of the input characteristics, saturation charge density on the belt is realized irrespective of the geometry of the ground end spraying comb C_1.

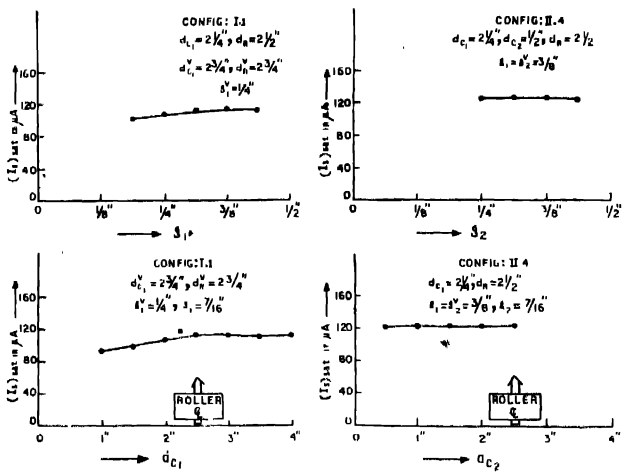

Fig. 4. Independence of saturation short circuit current for various comb geometries at the ground end.

(b) *High voltage end :*

The saturation short circuit current $(I_S)_{sat}$ was found to be insensitive with gaps $g_1{}^V$ and $g_2{}^V$ as shown in figure 5. Dependence of $(I_S)_{sat}$ on $d^V{}_{C_1}$ for configurations I.1, I.2, III.1, III.2, & IV.2a are shown in figure 6. The maximum $(I_S)_{sat}$ is about 120 μA in all these cases except in the configuration I.2.

In configuration I.1, both positive charge collection and negative charge spraying is present. The rise in $(I_S)_{sat}$ with $d^V{}_{C_1}$ is due to increased negative charge spraying and $(I_S)_{sat}$ passes through a maximum as the position of the comb $C^V{}_1$ coincides with the roller centre line. The maximum $(I_S)_{sat} = 65\mu A$ in configuration I.2 is due to the collection of positive charges alone, since with the roller connected to dome negative charge spraying cannot occur. The fall in $(I_S)_{sat}$ as the comb $C^V{}_1$ moves towards the roller is due to the drop in the belt surface potential

near the comb which affects the charge collection. In case of configurations III.1 and III.2, $(I_S)_{sat}$ was found to be constant due to saturation in both the values of I_+ and I_-. The saturation is mostly due to the presence of CV_2. The increase in the roller to dome potential was achieved in the case of configuration III.2 with the help of the comb CV_1 connected to the roller which helped to increase the collection of charges by the roller. The drop from about 120 μA as the comb CV_1 approaches the roller centreline is due to the presence of additional needles directed roller from the comb CV_2 which tries to limit the dome to roller potential affecting the negative charge spraying. In this case the geometry is such that the roller to dome potential falls below the threshold value for negative charge spraying as CV_1 approaches the roller centre line.

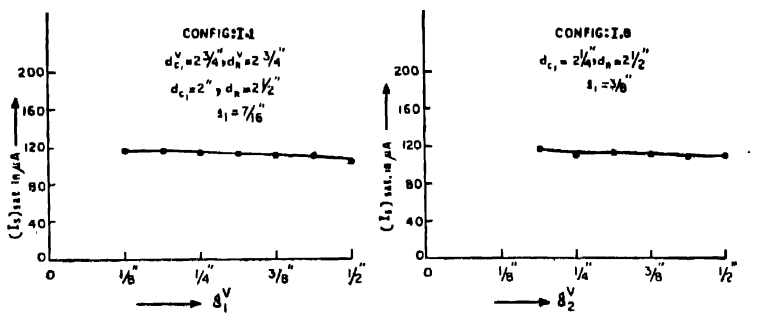

Fig. 5. Independence of saturation short circuit current with the gaps $g_1{}^V$ and $g_2{}^V$at the high voltage end.

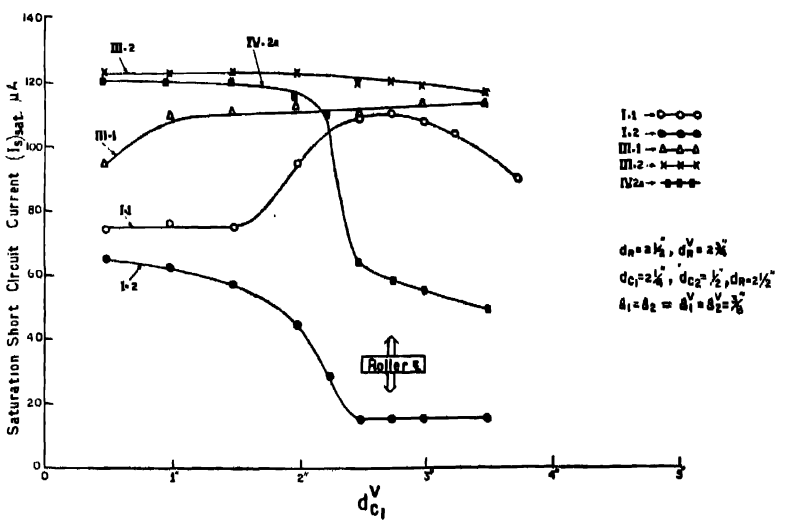

Fig. 6. Dependence of saturation short circuit current on dV_{C_1} for different comb configurations.

This particular aspect was studied in greater detail in configurations IV.3 and V.1. In case of IV.3 the roller to dome voltage was controlled by controlling the value of R_3, while in configuration V.1 the same was done by controlling the gap $g^V{}_3$ between the control comb CV_3 and the dome. The effect of roller to dome voltage on negative charge spraying is evident from the results shown in figure 7 while the collection of positive charges remained unaffected. Similar results are obtained in both the cases and this can be utilized for the control of downward and hence the total output current of the generator.

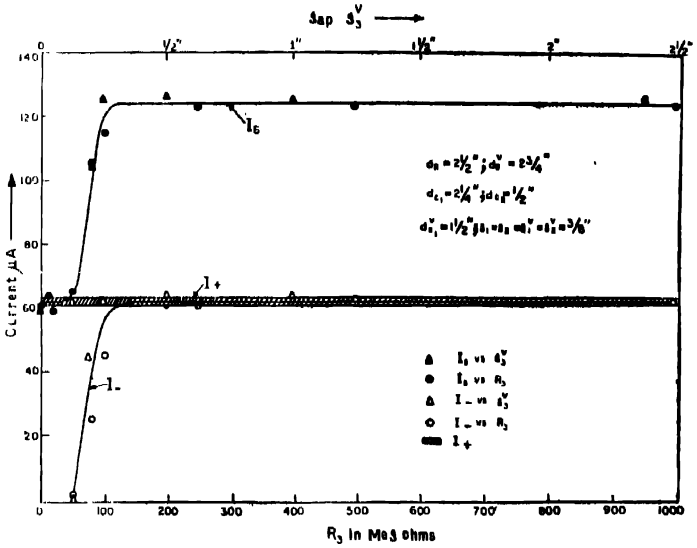

Fig. 7 Dependence of I_S, I_+ and I_- on dome to roller potential controlled by (i) resistance R_3 and (ii) the gap $g_3{}^V$ of the control comb C_3V. (The abscissa represents equivalent dome to roller voltage in arbitrary units.) The curves show that the control is achieved on I_- leaving I_+ unaffected.

3. Conclusion

Of all the configurations studied, configuration IV.2 was found to be the most convenient. It has the advantage of (i) maximum charge transfer under optimum geometrical conditions, (ii) reduced loading on the spray power supply, and (iii) control and stabilization of the roller to dome voltage. This control and stabilization of the roller to dome voltage was achieved through the use of a few additional adjustable needles from the comb CV_2 directed onto the roller without the actual presence of the additional comb CV_3 of configuration V.1 or the resistance R_3 of configuration IV.3..

Under the conditions of optimum charge transport we obtained a maximum short circuit current $\sim 120\ \mu A$. This corresponds to a charge carrying efficiency (Craggs & Meek 1954) $\sim 75\%$ of theoretical maximum.

Acknowledgment

We are grateful to Prof D. N. Kundu, Director of this Institute, for his kind interest and support. We are thankful to Dr. A. Chatterjee for timely advice and to Dr. N. K. Majumdar and Dr. S. K. Ghosh for helpful discussions. We also wish to thank Mr. A. N. Sinha, Mr. H. K. Das, and Mr. K. C. Paul for assistance and technical help.

References

Chatterjee A., Ganguly A, Ghosh S. K., Majumdar N. K., Mukherjee S., Saha A. & Sarkar R. 1973 *Science and Culture* **39**, 136.

Graggs J. D. & Meek J. M. 1954 *High Voltage Laboratory Technique*, Butterworths Scientific Publications, London, pp. 37-53.

Ganguly A. K. & Saha A. 1973 *Nuclear Physics & Solid State Physics Symposium*, Bangalore, India.

Herb R. G. 1959 *Handbuch der Physik* **44**, 64.

Livingston M. S. & Blewett J. P. 1962 *Particle Accelerators*, McGraw-Hill.

Smee J. F. 1944 *J. Inst. Elect. Engrs.* Pt 1, **91**, 422.

Van Atta L. C., Northrup D. L. Van Atta C. M. & Van de Graaff R. J. 1936 *Phys. Rev.* **49**, 761.

Van de Graff R. J., Trump J. G. & Buechner W. W. 1946-47 *Rep. Prog. Phys.* **11**, 1.